

Review on MRR in Spark Erosion Machining (SEM) Through ANN

Rahul Shrinivasan, Tushar Bhakte
IIT Kharagpur, West Bengal, India

ABSTRACT

EDM is a modern machining technology used to machine hard material pieces that are difficult to produce using traditional machining methods. This article aims to optimize process factors to obtain maximum MRR and high surface integrity in the end cut. Using artificial neural networks, this research proposes a technique for automatically determining and optimizing processing parameters in the EDM sinking process (ANN). The availability of machining data in the industrial tool room survey is the primary issue regarding adjusted process parameters for precision machining. Experiments are conducted to investigate the effect of pulse current, pulse on time, electrode area, and gap voltage on MRR response.

Keywords : Electricity fluctuation, operation, profitability, SMEs, Ghana.

Article Info

Volume 9, Issue 1

Page Number : 218-237

Publication Issue

January-February-2022

Article History

Accepted : 05 Feb 2022

Published : 11 Feb 2022

I. INTRODUCTION

Manufacturing industries are facing challenges from advanced difficult-to-machine materials, such as superalloys, ceramics, and composites, as well as stringent design requirements (high surface quality, high precision, high strength, complex shapes, high bending stiffness, good damping capacity, low thermal expansion, and better fatigue characteristics) and machining costs in this technological era. In recent years, there has been a rising tendency toward the usage of lightweight and compact mechanical components; as a result, there has been an increased interest in advanced materials in modern-day industries. Electric discharge machining is a novel manufacturing technique based on the electrothermal phenomena of material degradation. In the presence of dielectric fluid, a succession of discrete sparks between the tool electrode and the workpiece

removes the material. Because the tool does not contact the workpiece, the surface texture is devoid of tensions and cutting force imprints. EDM is ideal for machining forging dies, injection molds, and automotive components.

The solution may be avoided, and the training pace can be increased. The experiment demonstrated that using mirror processing conditions provided by the above approach will result in good small-area mirror processing outcomes and the necessary processing precision and efficiency. Trias Andromeda, AzliYahya, Nor Hisham, Kamal Khalil, and Ade Erawan present a prediction of Material Removal Rate (MRR) in Electrical Discharge Machining (EDM) using Artificial Neural Network for High Igap current in their research paper Predicting Material Removal Rate of Electrical Discharge Machining (EDM) using Artificial Neural Network for High Igap current (ANN). Die sinking EDM process data for copper-

electrode, and steel workpieces were collected. The goal is to create a behavioral model based on an input-output pattern of raw data from the EDM process trial. The behavioral model is used to forecast MRR, compared to the actual MRR number. The results demonstrate a high degree of agreement in forecasting MRR.

Markopoulos, Angelos P. In this study, Artificial Neural Networks (ANNs) models for predicting surface roughness in Electrical Discharge Machining are developed (EDM). Two well-known programs, Matlab with accompanying toolboxes and Netlab, were used for this purpose. The models were trained using data from many EDM tests on steel grades; the suggested models employ the pulse current, pulse length, and processed material as input parameters. The findings show that the proposed ANNs models can accurately predict surface roughness in EDM. Furthermore, they might be essential instruments for EDM Machining process planning. The ability to create complicated geometries and detailed designs with great precision, particularly when combined with CNC, makes it more precise and superior to any other machining technology. Despite all of these advantages, the EDM machine has certain disadvantages. One of the most prevalent difficulties that waste time is the removal or erosion of electrode material from the electrode. As we all know, the EDM process works by eroding the material or workpiece caused by the spark formed between the electrode's surface and the workpiece. Thus, the MRR is defined as the ratio of the weight difference between the workpiece before and after machining to the machining time and material density. The material removal rate impacts both the machining rate and the rate of tool electrode wear. MRR is the better-the-higher performance metric. The goal of this research is to acquire and analyze optimum parameters such as pulse on current (I_p), pulse on time (T_{on}), and gap voltage (V_o) that determine the output parameter Metal Removal Rate (MRR), and

therefore perform screening using Artificial Neural Networks. The following goals are given below -

- To simulate the material removal rate of the EDM machining process under optimal conditions.
- Research of a contemporary mathematical tool, the Artificial Neural Network.
- Machine parameters to provide a carbon-free surface. MRR optimization in relation to the depth of cut. Suggest an ANN model for process optimization and validation.

The new manufacturing model employs unconventional energy sources such as sound, light, mechanical, chemical, electrical, electrons, and ions. The machining techniques are unconventional because they do not use standard metal removal tools and instead rely on alternative types of energy. EDM has been utilised to create sophisticated materials with the desired form, size, and precision in recent years. EDM is a non-traditional machining technology that uses carefully controlled sparks between an electrode and a workpiece in the presence of dielectric fluid to manufacture electrically conductive materials. It employs thermoelectric energy sources to machine exceedingly poor machinability materials; its unique features include sophisticated intrinsic-extrinsic shaped tasks independent of hardness. One of the primary benefits of the EDM method is the ability to machine any electrically conductive material, regardless of hardness, using heat energy. EDM eliminates mechanical strains, chatter, and vibration difficulties during machining since it does not make direct contact (an inter-electrode gap is maintained throughout the operation) between the electrode and the workpiece. There are other types of EDM processes available. Still, this article is concerned with die Sinking (also called ram) type EDM machines. Numerous input machining parameters can be wide-ranging in the EDM process and have diverse impacts on the EDM performance characteristics. EDM has gradually replaced traditional machining techniques

and is now a well-established machining solution in many manufacturing industries worldwide. Modern EDM, which was created in the late 1940s, is now widely acknowledged as a standard production method worldwide. Sir Joseph Priestley, an English scientist, uncovered the history of EDM methods. It took more than a century to put some practical applications to use. In the previous sixty years, the popularity of this machining has expanded by leaps and bounds.

1.1 Types of EDM

There are three different types of EDM

- Die Sinking EDM
- Micro Electro Discharge Machining (MEDM)
- Wire Electro Discharge Machining (WEDM)

a. **Die Sinking EDM:** The most fundamental is EDM, a non-contact machining method in which metal is removed by a sequence of regular electrical discharges between a tool-workpiece submerged in an insulating liquid and coupled to a suitable power source. Figure 1.1 depicts a schematic representation of such a machine. For cutting poor machinability materials, it employs thermoelectric energy sources.

b. **WEDM:** It employs a thin single-strand metal wire (diameter 0.1 mm, often made of steel, brass, or copper) that cuts the workpiece during the operation. Deionized water is utilized as a dielectric, immediately pumped around the wire while filters and de-ionizer devices regulate its resistivity and other electrical characteristics. As a result, WEDM is frequently employed when minimal residual stresses are sought. In WEDM applications, the wire functions nearly like an electrical saw, with the ability to achieve very narrowly cutting angles. The machining quality, i.e., accuracy and surface rugosity, is closely connected to the discharge parameters (current, voltage, discharge time, polarity) and dielectric

cleanliness. Sparks with low current form little craters: the surface rugosity is modest, but so is the clearance rate.

- c. **MEDM** is a powerful bulk micromachining method that produces complex 3-D features with high-precision positioning steps. It applies to all metals and alloys and any electrical conductor. MEDM's distinct characteristics and large material base have led to the technique used in industrial applications such as micro-mechanical tooling, ink-jet nozzle fabrication, and micro-machining of magnetic heads for digital VCRs. MEDM was initially used to create microscopic holes in metal foils, but it is now employed in various applications.

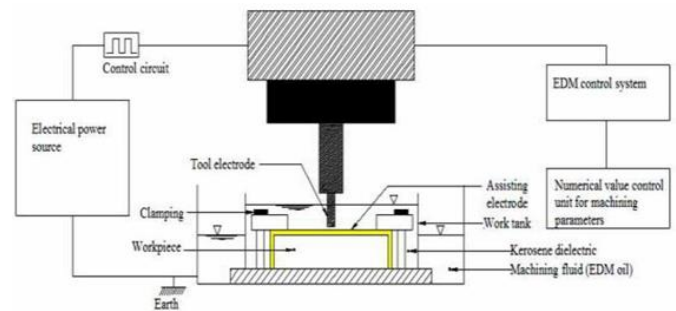


Figure 1.1 : EDM Schematic

1.2 Equipment of EDM

- **Dielectric system:** Dielectric fluid, delivery device, pumps, and filters comprise the dielectric system. Material removal in EDM is primarily caused by thermal evaporation and melting, which must be performed without oxygen to regulate the process and avoid oxidation. As a result, the dielectric system must provide an oxygen-free machining environment.
- **Electrode:** It is the instrument that determines the geometry of the created cavity. The material and design determine it. Selection criteria include: being widely accessible, easily machinable, having minimal wear, being electrically conductive, and having a good surface quality. The following electrode materials are frequently used in industry:

- Graphite
- Electrolytic oxygen-free copper
- Tellurium copper 99% Cu + 0.5% tellurium
- Brass

iii. Servo System: It is commanded by signals from the gap voltage sensor system in the power supply and regulates the electrode or workpiece in-feed to match material removal.

iv. Power Supply converts the alternating current from the main utility electrical supply to the pulse D.C. needed to generate spark discharges at the machining gap.

1.3 Working Principle of EDM

Figure 1.2: (a) Pre-breakdown phase (b) Breakdown phase (c) Discharge phase (d) End of the discharge and (e) Post-discharge phase

The essence of the EDM process is the conversion of electrical energy into heat energy via a succession of discrete sparks that occur between the tool electrode and a conductive workpiece submerged in a dielectric medium and separated by a tiny gap. Short-duration discharges are created in a liquid dielectric gap that separates the tool and the workpiece. Electrical energy is required to develop the electrical spark, and heat energy is used to remove the material in this process. The electrode is brought closer to the workpiece until the gap is narrow enough to ionize the dielectric. The dielectric flush eroded particles from the gap, and it is critical to keep this flushing going indefinitely. Because the workpiece is held in position by the fixture arrangement, the tool aids in concentrating the discharge or intensity of produced heat at the location of shape disclosure. Heat elevates the temperature of the workpiece in the region of tool position, melting and evaporating the metal. The machining process eliminates tiny quantities of workpiece material through the mechanism of melting and vaporization during a discharge. The erosion process in EDM is commonly divided into the following phases, depicted in Fig. 1.2.

i. Pre-breakdown: During this phase, the electrodes are kept at a small distance apart, with the electrode moving close to the workpiece and a large potential difference applied between the electrodes.

ii. Breakdown: The dielectric breakdown occurs when the applied voltage exceeds the strength limit of the utilized dielectric fluid. The breakdown site is usually between the electrode and the workpiece, but it can also be caused by conductive particles or debris in the gap. When a breakdown occurs, the voltage drops, and the current rapidly increases. During this phase, the dielectric becomes ionized, resulting in a plasma channel between the electrodes.

iii. Discharge: During this phase, the discharge current is kept constant to allow for a continuous attack of ions and electrons on the electrodes, resulting in high heating of the workpiece material and a temperature rise of between 8,000 C and 12,000 C. This quickly leads to the formation of a tiny molten metal puddle at the surface of the electrodes. Due to the great heat, a small amount of metal is also instantaneously evaporated. The plasma channel extends during this phase; hence the radius of the molten metal pool grows with time. Throughout the discharge process, the Inter Electrode Gap is a critical metric.

iv. End of the discharge: During this phase, the current and voltage supplies are turned off, causing the plasma to collapse under the pressure exerted by the surrounding dielectric.

v. Post-discharge: There will be no plasma during this period. Because the plasma is contracting and cooling, a little part of the metal will be machined, and a slight thin coating (white layer) will be deposited. As a result, the molten metal pool is sucked up into the dielectric, leaving a small crater on the workpiece surface.

Finally, the machining process eliminates tiny volumes of workpiece material that become molten or vaporized after a discharge and is taken away from the inter-electrode gap in the form of debris by the

dielectric flow. After material removal at the point of spark, the gap widens, and the position of the next spark changes to a new location on the workpiece surface where the gap is lowest. According to the inter-electrode gap, thousands of sparks erupt at different locations throughout the whole surface of the workpiece. As a result, a workpiece duplicate of the tool surface form is created.

1.4 EDM Process Parameters

Because of the differences in design, each EDM machine has a unique set of parameters. It is necessary to identify essential process factors that determine the reactions listed below to execute effective machining. The machine defines the entire collection of settings. The machining parameters are classified as follows: Input /process parameters: Voltage (V), discharge current (I_p), pulse-on time (T_{on}), pulse-off time (T_{off}), duty factor (τ), flushing pressure (F_p), workpiece material, tool material, inter-electrode gap (IEG), Lift Time (T_{up}), Work Time (T_w), and polarity (p) are the parameters that affect the machining process's performance.

- i. Gap Voltage: The voltage of applied pulses that determines the spark energy is specified by open-circuit voltage. Before current flow, this deionizes the dielectric medium, dependent on the electrode gap and dielectric strength.
- ii. Pulse-on time: The amount of time that real machining takes place or the amount of time that electricity is permitted to flow every cycle. The longer the pulse length, the greater the spark energy, which causes broader and deeper crevices. This is because the amount of material removed is proportional to the amount of energy delivered on time. The gap state determines the lengths of the ignition delay and discharge duration during pulse duration. Pulse duration and discharge current assess the energy created during a single electrical discharge.
- iii. Discharge current: The current rises until it reaches a certain level, denoted as discharge current.

The number of power units connected parallel to the gap is generally determined by the discharge current on static pulse generators. The higher the power intensity during electrical discharge, the greater the discharge current. It is the essential EDM machining characteristic related to power consumption when milling.

- iv. The effective area of electrode: The effective tool area is the area eroded by the tool surface comparable to the tool area of the blind cavity. The tool area's influence is inversely proportional to the MRR. As a result, a cavity with a smaller electrode area will result in a greater depth of cut.
- v. Duty cycle: It is the proportion of on-time to total pulse period. With a higher duty cycle, the spark energy is delivered for a longer length of the pulse period, resulting in greater machining efficiency.
- vi. Pulse-off time: The amount of time between sparks during which the supply voltage is switched off, causing the discharge current to drop to zero. During this period, the molten material solidifies and is washed out of the arc gap. This is setting influences the cut's speed and stability. As a result, if the cut-off period is too short, it will result in unsteady sparks.
- vii. Polarity: It describes the potential of the workpiece concerning the tool; depending on the application, the polarity might be either positive or negative. Carbide, Titanium, and copper are commonly cut using a negative polarity.
- viii. Inter Electrode Gap: The distance between the electrode and the component is during the EDM process. It's also known as a spark gap. It is one of the most critical needs for spark stability and flushing. The average gap voltage can estimate gap width, which is not directly measured. The tool servo mechanism is in charge of keeping the working gap at a constant value.
- ix. Dielectric fluid: The dielectric fluid serves as an electrical insulator in the EDM for the most critical reasons. Paraffin, deionized water, light transformer oil, and kerosene are the most utilized dielectric fluids. It cools the electrodes, creates a high plasma pressure

and a strong removal force on the molten metal, and aids in flushing these eroded particles away.

x. Flushing pressure: Flushing is the process of introducing clean, filtered dielectric fluid into the machining zone in EDM. If the cavity is deeper, the flushing becomes more difficult; ineffective flushing may cause arcing and the formation of undesired cavities, which can ruin the workpiece. There are numerous ways for flushing the gap that is often used: injection flushing, suction flushing, side-flushing, motion flushing, and impulse flushing. The typical pressure range is between 0.1 and 0.4 kg/cm².

xi. Lift time: It is the time when the tool is lifted, and the Inter Electrode Gap is flushed.

II. METHODOLOGY

2.1 Procedural Steps

- Referring research paper to know the most influential parameters of EDM.
- Understanding and forming optimal sets and combinations of input parameters.
- Collecting experimental data for developing neural network model.
- Understanding and developing ANN model with the best suitable algorithm.
- Collecting experimental data for validation and prediction purposes for the developed ANN model.

Figure 2.1: Procedural Steps

2.2 APPLICATION OF ARTIFICIAL NEURAL NETWORK TO PREDICT MRR OF EDM

In the past two decades, neural networks have been highly flexible modeling tools to learn the mathematical mapping between input and output variables for nonlinear systems. An artificial Neural Network (ANN) is an algorithm that imitates human beings' biological nervous systems. It has certain performance characteristics in common with biological neural networks. It comprises a huge

number of highly linked processing components (neurons) that work together to solve issues. ANNs, like humans, learn by doing. An ANN is trained for a specific application through a learning process, such as pattern recognition or data categorization. In biological systems, learning entails changes to the synaptic connections between neurons. The main objective is to model the EDM process for optimum operation representing a particular problem in the manufacturing environment where defining the optimization objective function using a smooth, continuous mathematical formula is impossible.

2.3 TRAINING THE EXPERIMENTAL DATA FOR ANN

Experiments were conducted to gather data for training or learning for neural network purposes. The training data set includes many cases, each containing values for a range of input and output variables. The first decisions will be needed: which variables to use and how many (and which) cases to gather. The choice of variables (at least initially) is guided by intuition. The researcher's expertise in the problem domain will give some ideas of which input variables are likely to be influential. The EDM process was conducted using copper electrode and steel workpiece materials. Experimental results of the material removal rate were recorded and presented in tabular form. The gap voltage V_{gap} falls to about 30V, 35V, 40V, and 45V, and the gap current rises to a selected constant value. The gap currents were selected at 3A, 5A, 7A, and 10A. A value for the material removal rate constant has been identified based on the empirical Analysis carried out on the experimental data and compared with the simulation result from the model using the Matlab software tool.

2.4 Collecting experimental data for validation and prediction purposes for the developed ANN model.

Although, the network successfully derived the complex relationship between the input values and MRR of the EDM process. After successful network training, it is expected to have mapped the desired relationship between the various input and output parameters. The network should also generalize this relationship for its application for new problems. The validation can be concluded that there is good agreement between network predicted and experimental results. Hence, it can be concluded that this ANN model serves as a good model for predicting MRR.



Figure 2.2: Flow Chart of ANN Architecture

III. EXPERIMENTAL SETUP

This chapter discusses the project's experimental setup. In this chapter, light is thrown on various aspects such as the machines used, their specifications, materials used for the experimentation, the laboratory

used, etc. This chapter gives the importance of the various machines used and their applications. This chapter also enlightens the composition and various properties of the material used in the experimentation. Besides the main experimental setup, other machines and tools were used to complete the experiment.

3.1 Laboratory used

Table 3.1: List of the laboratory and machines used

Sr. no Laboratory Machine

1. Workshop Electric Discharge Machine Automatic hack saw Grinder
2. Metallurgy lab Rockwell Hardness tester

3.2 Machines used

The various machines used in this project are as follows

3.2.1 Electric discharge machine

This machine is the soul of this project. All the experimentation of the project is carried out on this machine. It works on the principle of spark erosion, as discussed earlier. Figure 6.1 shows the actual setup of the electric discharge machine (EDM).

The specifications of the electric discharge machine (EDM) are given in table 6.2. The EDM machine is a non-conventional type of machine which finds its applications in mold-making industries.

Table No. 3.2:EDM Machine Technical Specification:

Size of Machine	Length X Width X Height	1250 X 1800 X 1100 mm
Work Head	Travel of the Quill	150 mm
Technical Data		
Co-ordinate Table	Mounting Surface(Length x Width)	400 X 250 mm
	Maximum Workpiece Height :	200mm
	Maximum Workpiece Weight:	200Kg
	Longitudinal Travel (X-Axis)	240mm
	Transverse Travel (Y-Axis)	150mm
	Maximum Table-Z-slide spindle distance universal axis:	325mm
	Minimum Table-Z-slide spindle distance universal axis	150mm
Work tank size	Length X Width X Height	685 X 445 X 290mm
	Motor Specification	0.5HP, 0.37KW,
		415V, 3 Ph, 50 Hz

3.3.1 Workpiece material

D2 steel is a high-carbon, high-chromium tool steel that hardens in the air. It is very worn and abrasion-resistant. It is heat treatable, with a hardness range of 55-62 HRC, and is machinable in the annealed state.

When adequately hardened, D2 steel exhibits low deformation. Because of its high chromium content, D2 steel has mild corrosion resistance when hardened.

Table No. 6.3: Thermal Properties for Cu.

Sr. No.	Properties	Values
1	Thermal conductivity	386 (W/m K)
2	Specific Heat	0.383 (J/gm K)
3	Latent heat of Melting	133 (J/gm)
4	Latent heat of Vaporization	5066 (J/gm)
5	Melting Temp.	1063(°C)
6	Boiling Temp.	2562(°C)

6.3.2 Tool electrode material

Copper is the most commonly used EDM tool material against En31 as workpiece material. Copper is selected as the tool material. A square tool was taken for experiments. Figure 6.3 shows the actual tool electrode with their cross-section, and table 6.4 consists of properties and dimensions of the copper electrode, respectively.



Figure 6.3 : Square Tool

6.3.3 Dielectric Fluid

In EDM, the dielectric fluid provides three essential functions.

- To insulate the gap between the inter-electrodes.
- To remove debris from the machined area.
- Serves as a coolant to aid in heat conduction between the electrodes

Table No. 6.5 : Properties of EDM Oil.

Sr. No.	Property	Value
1	Viscosity	15.4*10 ⁻⁶ (m ² /s)
2	Thermal Diffusivity	70.7*10 ⁻⁹ (m ² /s)
3	Thermal Conductivity	0.110 (W/m K)

EDM EXPERIMENTATION -

A. The trials were carried out using a die-sinking EDM machine of Electronica E-20 with a pulse generator. Under jet flushing, the dielectric fluid pressure is 3.1kgf/cm². The experimental workpiece material is AISI D2 alloy steel, employed in the inner core and parts of cold-work dies and molds. Furthermore, the copper tool is chosen in a prismatic shape with a transverse area of 15mm 15mm and a height of 50mm. As tool electrodes, copper rods with 98 percent purity and 8.94 g/cc density were machined with an excellent surface polish and accurate dimensions. Copper electrodes and workpieces were meticulously honed to ensure stable machining conditions throughout the EDM process.

B. Design of Experiments –

A sequential incremental design method was used. The type of variation in response to a given factor aids in determining the factor's levels. Though there are many parameters involved in the EDM process, the level of the generator current pulse intensity (Ip), pulse time (Ton), and gap voltage (Vg) have been taken into account as design elements in this study. Table 1 shows the parameter levels that correspond to each other.

Table 1: Machining parameters with levels

Symbol	EDM machining parameters and levels	Levels			
		1	2	3	4
Ip	Pulse Current (amps)	3	5	7	10
Ton	Pulse-on Time (sec)	0.11	0.17	0.29	0.38
Vg	Gap Voltage (volt)	130	135	140	145
Ae	Gap Voltage (volt)	L10 x W10	L15 x W15	L17 x W17	L20 x W20

C. Response Variable –

MRR The content MRR is defined as the ratio of the weight difference between the workpiece before and after machining to the machining time and material density. The material removal rate impacts both the machining rate and the rate of tool electrode wear. MRR is the better-the-higher performance metric. It is commonly represented in millimeters of water per minute (mm³/min).

D. Artificial Neural Network (ANN)

An artificial network comprises a collection of small processing units that communicate with one another by delivering signals via a large number of weighted links. Using the program MATLAB, a variety of ANN models were trained to simulate the performance characteristics of the EDM process. ANN designs, learning/training procedures, and the number of hidden neurons are frequently modified to produce an improved prediction model, but the adjustments are performed at random. So, a sequential incremental design was used for the experiment design to attain the best of the above for modeling and solution. The data collection is separated into three sections in the ratio 1/2: 1/4: 1/4. With 1/2 of the data used for training, 1/4 for testing, and 1/4 for validation of the network

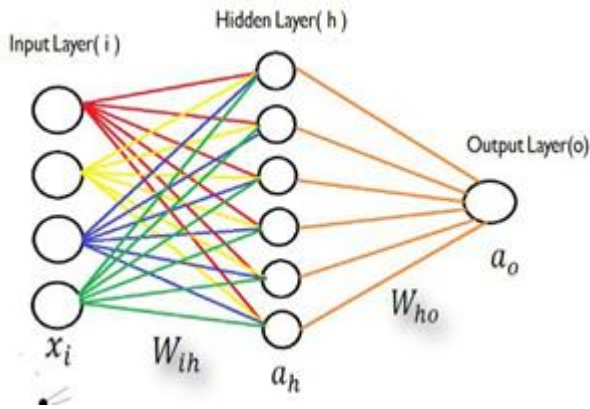
chosen at random by MATLAB's nntool. In this paper, Md. Ashikur Rahman Khana discusses how modeling may aid in the development of a better knowledge of such complicated processes, reduce machining time, and make the process more cost-effective. As a result, the current study focuses on creating an artificial neural network (ANN) model.

IV. RESULTS AND ANALYSIS

Table 2 displays the experimental data for surface roughness in finish cut machining for AISI D2. The factors studied in the tests include current intensity (I_p), pulse on time (T_{on}), and gap voltage (V_g), and the behavior of each parameter has a substantial impact on surface roughness. Table 2 shows the results of the experiment

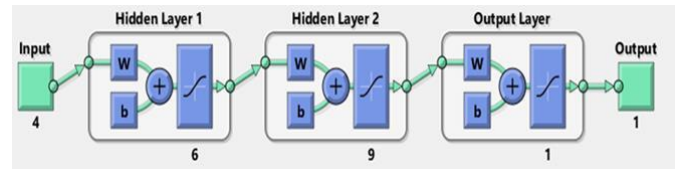
Table 2: Experimental Output

S. No.	I_p (amp)	T_{on} (sec)	V_g (volt)	A_e (mm ²)	MRR (mm ³ /min)
1	3	0.11	130	L10x W10	5.1948
2	3	0.17	135	L15x W15	7.4458
3	3	0.29	140	L17x W17	4.2424
4	3	0.38	145	L20x W20	6.0317
5	5	0.11	135	L17x W17	6.9062
6	5	0.17	130	L20x W20	4.2343
7	5	0.29	145	L10x W10	8.8311
8	5	0.38	140	L15x W15	10.505
9	7	0.11	140	L20x W20	3.3697
10	7	0.17	145	L17x W17	2.7705
11	7	0.29	130	L15x W15	1.6161
12	7	0.38	135	L10x W10	10.851
13	10	0.11	145	L15x W15	13.823
14	10	0.17	140	L10x W10	13.391
15	10	0.29	135	L20x W20	2.7417
16	10	0.38	130	L17x W17	6.5800



A. Training Neural Network Using Matlab

The sequential incremental technique was used to choose the optimal process parameter setting for ANN modeling. Gradient Descent with Momentum and Adaptive Learning Rate (GDX) training technique, 6 hidden neurons in first hidden layer, 9 neurons in the second hidden layer, and MLP neural architecture were chosen as ideal process parameters. Because this run's weights and bias matrix had the lowest MSE and highest R-value, they were used to simulate MRR. As a result, the architecture 4-6-9-1 was chosen and trained in Matlab using nntool.



B. The Analysis of MRR

Table 3 contains the values of the ANN output data for validation and comparison. R=0.96753 was discovered to be the correlation factor for all of the data. Figure 5 depicts the variation of MSE of training, validation, and testing data sets with respect to the epoch. The validation data set is used to halt the training process early to provide improved generalization. Figure 7.6 indicates that at epoch 453, the validation error is at its lowest.

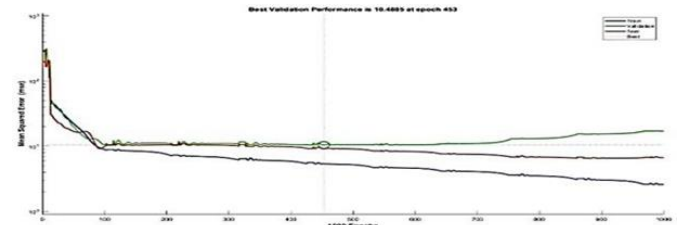


Figure 5: Variation of MSE w.r.t. epoch

Table 3: Experimental Output

S. No.	Ip amp	Ton sec	Vgvolt	Ae mm ²	MRR (mm ³ /min)
1	3	0.11	130	L10 x W10	5.16388 7
2	3	0.17	135	L15 x W15	7.42318 3
3	3	0.29	140	L17 x W17	6.97982 5
4	3	0.38	145	L20 X W20	5.03532
5	5	0.11	135	L17 X W17	7.88635 6
6	5	0.17	130	L20 x W20	5.61709 5
7	5	0.29	145	L10 x W10	8.70742 3

8	5	0.38	140	L15 x W15	9.67214 8
9	7	0.11	140	L20 x W20	2.74172 9
10	7	0.17	145	L17 x W17	2.74172 9
11	7	0.29	130	L15 x W15	3.52270 3
12	7	0.38	135	L10 x W10	12.9675 4
13	10	0.11	145	L15 x W15	18.9827 5
14	10	0.17	140	L10 x W10	16.2699 2
15	10	0.29	135	L20 x W20	4.17157 5
16	10	0.38	130	L17 x W17	8.59945 2

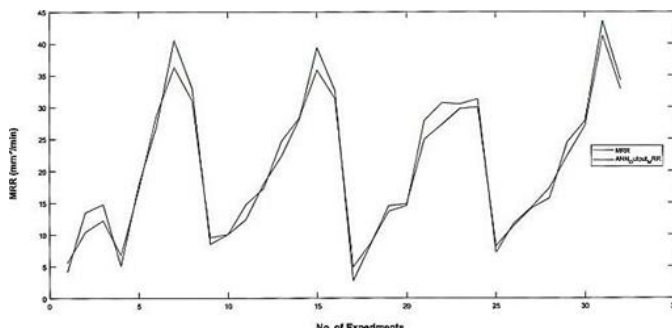


Figure 6: Comparison of Experimental output to ANN output

L20 x W20 and I_p for 3A to 4.5A (4-5) describes the fine cut machining region. The region enclosed for 5A till 7.5A (7-8) shows the transition from the fine machine cut to the rough cut machining. The cubic fitting polynomial has been used in the response surface plot of MRR, A_e , and I_p . The rough zone of the machining can be seen with the increase in current above 8A. Thus, a higher MRR can be obtained in the machine-prone region, compromising the surface finish of the work part.

A. Optimization and Comparison of MRR Responses

Cubic fit for MRR, A_e , and I_p

The surface plot (figure 6) for two variables simultaneously can be analyzed against MRR within the interval of finish cut to rough cut machining. The plot of MRR, A_e , and I_p the levels from L10 x W10 to

Cubic fit for MRR, I_p , and T_{on}

The surface plot (figure 7) for two variables simultaneously can be analyzed against MRR within the interval of finish cut to rough cut machining. In the plot of MRR, I_p , and T_{on} , the levels from 3A to 4.5A (4- 5) describe the fine cut machining region. The region enclosed for 5A till 7.5A (7-8) shows the transition from the fine

machine cut to the rough cut machining. The cubic fitting polynomial has been used in the response surface plot of MRR, I_p , and T_{on} . The variation of T_{on} as that compared to current is negligible. Thus, I_p is a dominant affecting MRR. The rough zone of the machining can be seen in the bright yellow zone with the increase in T_{on} above 290 μs and higher current values. Thus, a higher MRR can be achieved with an increase in T_{on} and increasing current in the machine-prone region, compromising the work part's surface finish.

Cubic fit for MRR, V_g , and T_{on}

The surface plot (figure 8) for two variables simultaneously can be analyzed against MRR within the interval of finish cut to rough cut machining. An inverse relationship between V_g and T_{on} in the plot of MRR, V_g , and T_{on} , an inverse relationship between V_g and T_{on} can be seen. Thus, the distinct observation for MRR keeping T_{on} as 110 μs can observe that with an increase in V_g , the steady transition from fine cut machining to rough machining zone. In contrast, for a higher value of T_{on} 380 μs (here), the transition from rough machining to a finish cut can be seen over the V_g range. The fine-cut zone of the machining can be seen in the dark blue region.

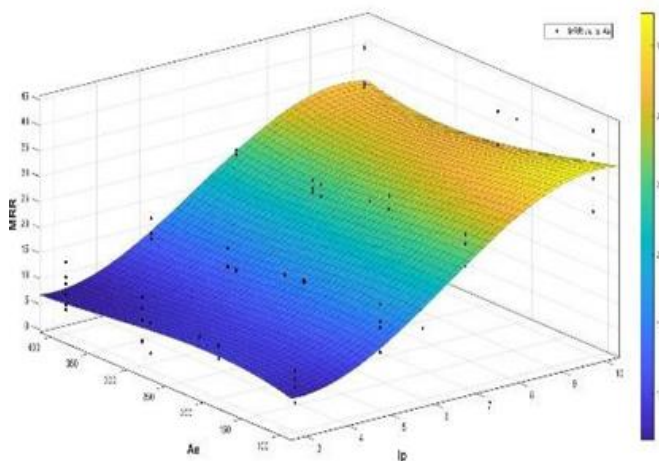


Figure 6: Cubic fit for MRR, I_p , and T_{on}

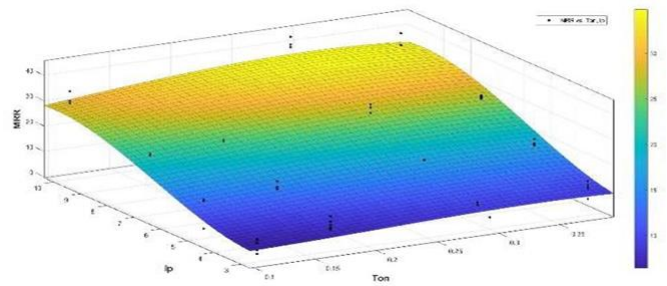


Figure 7: Cubic fit for MRR, I_p , and T_{on}

Figure 8: Cubic fit for MRR, V_g , and T_{on}

SURFACE TOPOGRAPHY

Surface topography is the study of geometrical features and spatial interactions and how component elements are interconnected or structured. Scanning electronic microscopy of the machined surface is used to analyze the surface topography of various samples. This chapter depicts the surface topography of the machined surface created on a D2 tool steel workpiece during EDM with a positive copper electrode for different discharge energies.

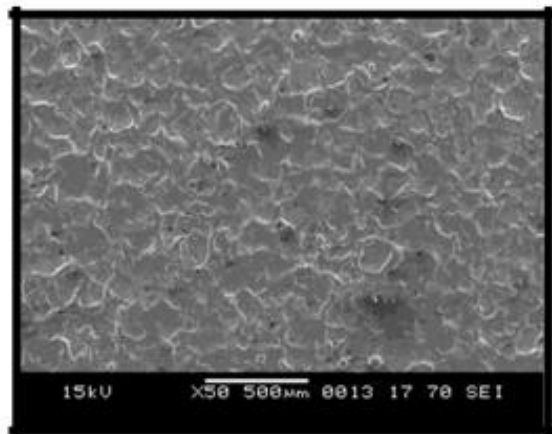
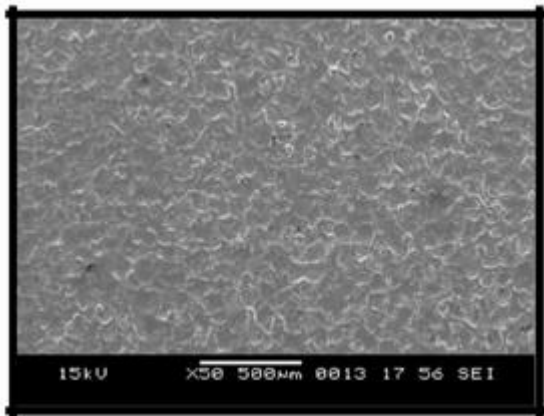
These figures show globules, craters, fissures, and tiny debris on the machined surface. The spark produced by the high-temperature plasma melts and vaporizes a tiny region of the workpiece surface, resulting in the formation of craters. The size of the crater is determined by the peak current and the discharge energy. At low peak current, small craters form. Less peak current and high frequency are associated with low material erosion, resulting in smaller craters.

Scanning electronic micrographs indicate the existence of fissures caused by the recast layer's solidification and/or quick cooling. Cracking is initiated by several surface defects in the recast layer created by the EDM process. The dielectric fluid rapidly cools the surface layer after the discharge and creates residual tensile tension. Cracks emerge when the residual tensile stress in the surface exceeds the material's ultimate tensile

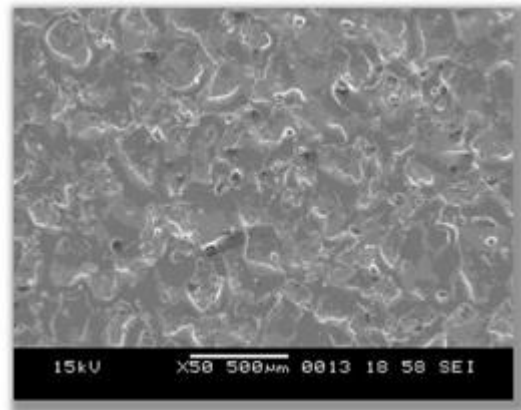
strength. Cracks do not form easily inside a thin recast layer because it dissipates heat quickly.

As a result, lesser discharge energy causes micro-cracks. Although most of the melted and vaporized material is flushed away by the dielectric after the pulse-on period, a tiny quantity of molten material is not ejected. After being rapidly cooled by the dielectric fluid, the unrepelled molten material resolidifies and produces globules of debris.

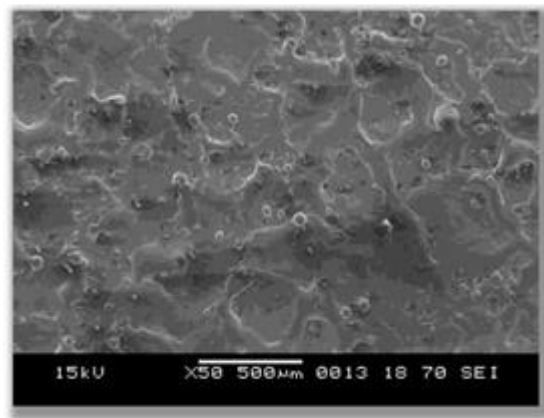
9.1 Variation of surface integrity concerning I_p (Images at x50 and 500 μm)



Low-Level Parameters



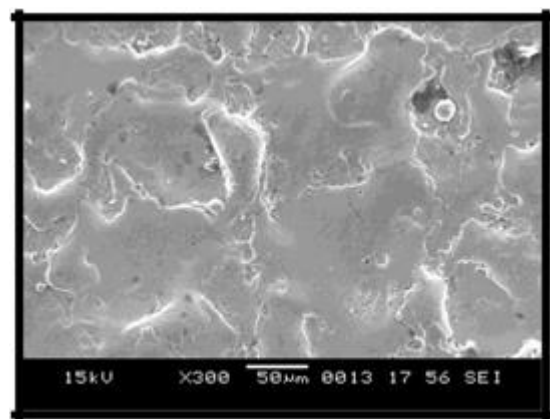
Img 9.1.13A

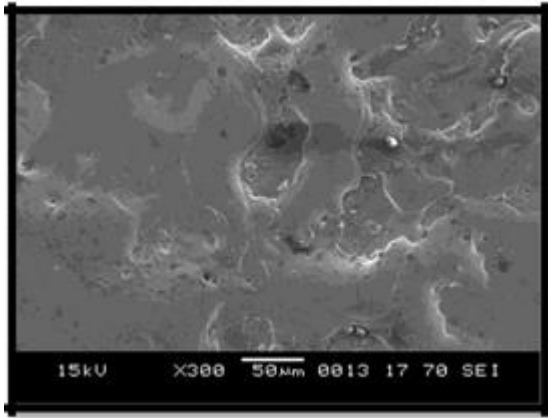


Img 9.1.2 5A

High-Level Parameters

Image 9.1.3 5A





Img 9.1.4 7A

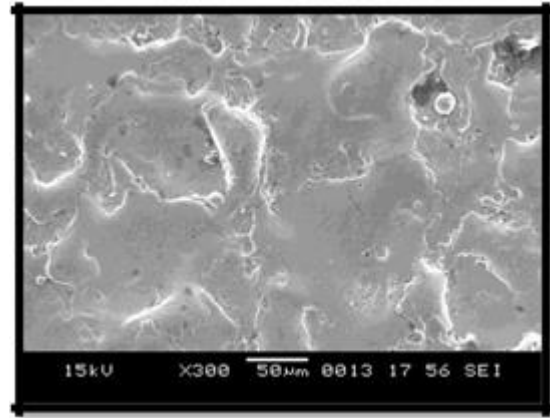
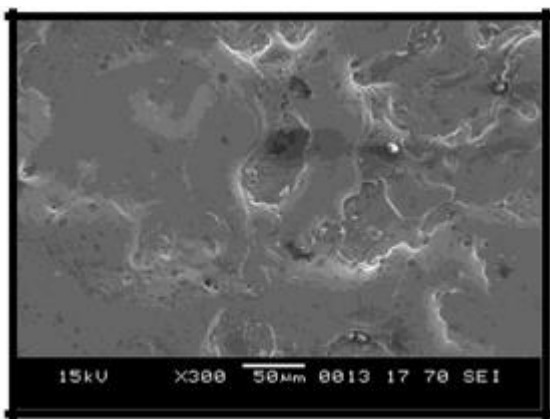
Discussion: As I_p increases, so does the discharge energy, which facilitates melting and vaporization of the workpiece material and creates larger and deeper craters, increasing surface roughness. The crater size grows larger with increasing current, and the surface texture gets rougher.

9.3 Variations of Cracks, Craters, and globules for different I_p and Ton

(Images at x300 and 50µm)

Low-Level Parameters

Img 9.3.1 3A



Img9.3.2. 5A

High-Level Parameters

Image 9.3.3. 5A

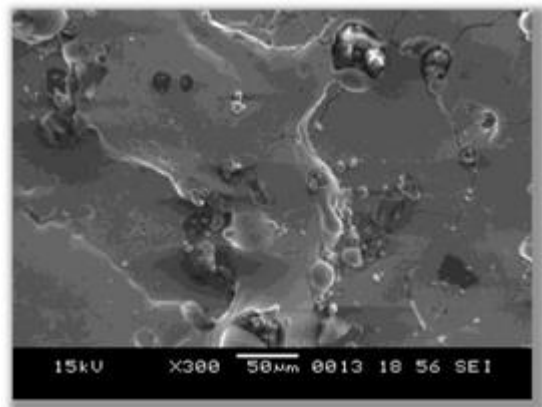
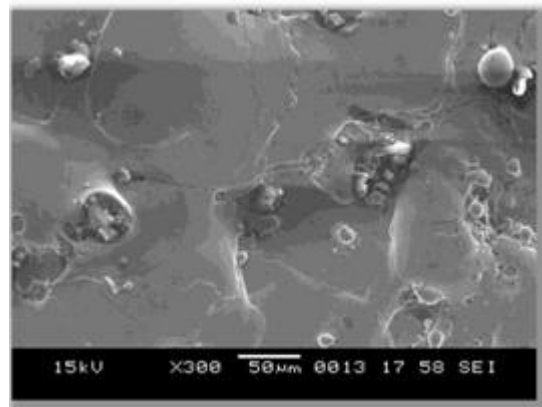


Image 9.3.4. 7A



Discussion: The discharge energy rises as the Ton increases. More craters are formed due to the increased discharge energy, which accelerates material degradation. As a result, as the Ton increases, the surface roughness does. However, a too-long Ton generates arcing and minimizes material erosion. Because of the expansion of the

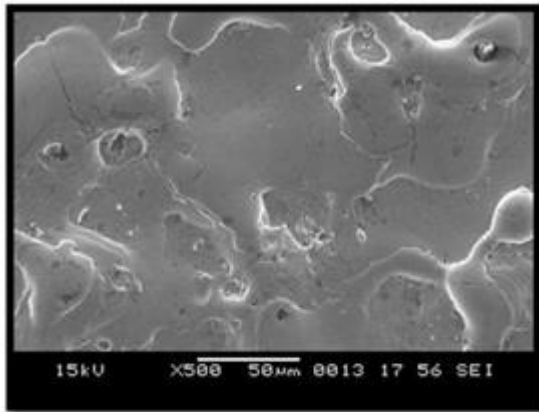
discharge column at a longer Ton, the energy density inside the discharge point is lowered. As a result, tiny craters are formed at too long Ton. As a result, a decreasing propensity to overly long Ton (about 290–380 s) is visible

9.4 Study of Cracks for different Ip Values

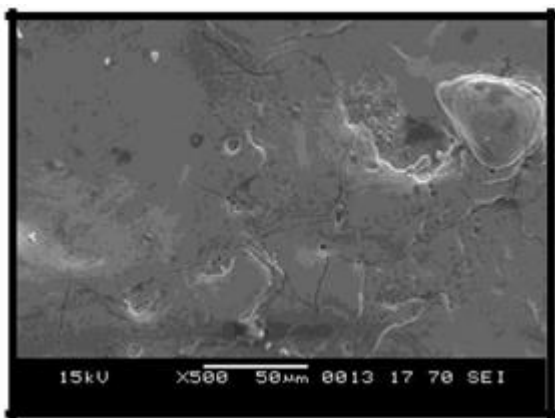
(Images at x500 and 50µm)

Low-Level Parameters

Img 9.4.1 3A



Img9.4.2. 5A



High-Level Parameters

Image 9.4.3. 5A

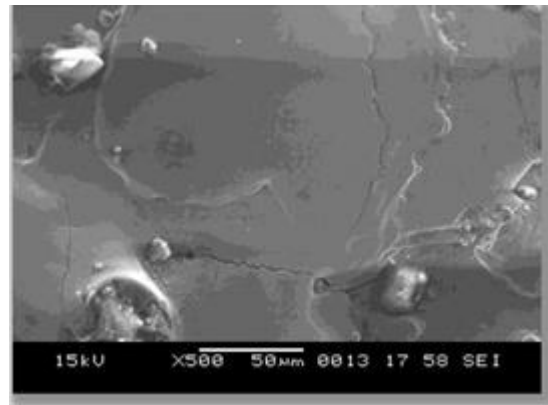
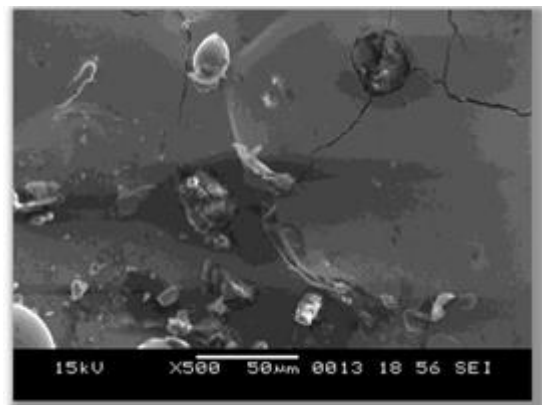


Image 9.4.4. 7A



Discussion: When only one of the subject materials' cracks and EDM parameters are evaluated, it is discovered that, for a constant pulse current, the surface crack density rises as the pulse-on time grows. If the pulse-on time is kept constant, the surface fracture density falls as the pulse current increases. When the pulse current increases, the thickness deviation steadily increases, as does the thickness ratio of the thick to the thin white layer.

V. CONCLUSION

The size of the craters rises as the discharge energy level increases, according to the SEM photos in Figures. It is discovered that when the energy level rises, the number of globules decreases. Furthermore, when the discharge energy increases, so does the degree of cracking. The high discharge energy generates intense sparks, an impulsive force that impact the surface. As a result, the melting and

vaporization rates rise, resulting in higher material removal. This results in bigger and deeper craters on the workpiece's machined surface. Long Ton is responsible for bigger craters, but strong Ip is responsible for deep craters during high energy levels. As a result of the tremendous discharge energy, deeper and broader craters form, resulting in a rougher surface. Recast layer thickness and generated stress are two elements that contribute to a higher degree of fracture development.

Furthermore, a high gap voltage provides for a shorter cutting time. As a result, increasing Vg minimizes material erosion, resulting in smaller craters. As Sv increases, surface integrity diminishes, and a higher servo-voltage value results in a more uniform surface on the workpiece.

The thickness of the recast layer grows in proportion to the discharge energy. Ton increases the thickness of the white layer and the residual stress. At long Ton, a greater quantity of heat energy reaches the inside of the workpiece. The temperature of the workpiece surface quickly surpasses the melting point. Following quick cooling by the dielectric fluid, the molten material resolidifies, resulting in a thick recast layer. As a result, the increased energy level causes more fractures—the high discharge energy results in forming an inhibitor carbon layer on the electrode surface. The carbon deposited on the electrode surface grows significantly as Ton increases. This carbon layer reduces electrode wear. Because of the high discharge energy, a considerable impulsive force may remove more debris from the machining gap. As a result, the surface topography with high discharge energy lowers the number of globules.

Crack formation is related to the EDM parameters. An increased pulse-on duration will increase both the average white layer thickness and the induced stress. These two conditions tend to promote crack formation. When the pulse current is increased, the

increase in material removal rate causes a high deviation of the thickness of the white layer. Compared to a thin white layer, it is true to say that a thick white layer tends to crack more readily. However, the area occupied by the thick layer is less, so the density of surface cracking is broadly similar for both thin and thick layers.

VI. FUTURE SCOPE

The future scope of the present work as understood in due course of performance of the project is enumerated as under:

- Experiments with workpieces of different materials can be investigated.
- Experiments with varying materials of tool can be done, and the current experiments can be compared.
- The effect of other process parameters like pulse on time, pulse off time, the voltage on the material removal rate, and different surface roughness parameters can be investigated.
- Apart from back-propagation learning for the modeling of the artificial neural network, another algorithm can be used to know if at all there is any better ANN model exists or not.
- Optimization techniques like a genetic algorithm (G.A.) response surface methodology (RSM) can be applied for this model optimization.

VII. REFERENCES

- [1]. ANN Performance evaluation in modeling of MRR in EDM Process by Shiba Narayan Sahu, Debasis Nayak, Hemanta Kumar Rana, 2003.
- [2]. Predicting Material Removal Rate of Electrical Discharge Machining (EDM) using Artificial

- Neural Network for High Igap current. Trias Andromeda, Azli Yahya, Nor Hisham, Kamal Khalil, Ade Erawan, 2011.
- [3]. Artificial Neural Networks Modeling of surface finish in Electro-Discharge Machining of tool steels by A. Markopoulos, N.M. Vaxevanidis, G. Petropoulos, D.E. Manolakos, 2006.
- [4]. Md. Ashikur Rahman Khana*, M. M. Rahmanb, K. Kadirgamab, Neural network modeling and Analysis for surface characteristics in electrical discharge machining (ICME 2013).
- [5]. J. Ghaisari, H. Jannesari, M. Vatani, Artificial neural network predictors for mechanical properties of cold rolling products, *Adv. Eng. Softw.* 45(2012) 91–99.
- [6]. Martin T. Hagan, Oklahoma State University Stillwater, Oklahoma .Neural Network Design, 2nd Edition, eBook.
- [7]. Investigation and Analysis of process parameters for spark erosion machining, Final year Project (2016-2017).
- [8]. Wang, K., Gelgele, H.L., Wang, Y., Yuan, Q., Fang, M., 2003, “A hybrid intelligent method for modelling the EDM process”, *International Journal of Machine Tools & Manufacture*
- [9]. K.H. Ho, S.T. Newman, 'State of the art electrical discharge machining (EDM)', *International Journal of Machine Tools & Manufacture* 43 (2003) 1287–1300.
- [10]. NorlianaMohd Abbas, Darius G. Solomon, Md. FuadBahari, 'A review on current research trends in electrical discharge machining(EDM)', *International Journal of Machine Tools & Manufacture* 47 (2007) 1214–1228.
- [11]. D.T. Pham, S.S. Dimov, S. Bigot, A. Ivanov, K. Popov, 'Micro-EDM—recent developments and research issues', *Journal of Materials Processing Technology* 149 (2004) 50–57.
- [12]. John, E., F., *Electrical discharge machining*, Rockwell International, ASM Metals Handbook, Vol. 16 Machining, pp. 557-564, 1997.
- [13]. Margaret, H., C., *Environmental Constituents of Electrical Discharge Machining*, thesis Submitted to the Department of Mechanical Engineering, Massachusets Institute of Technology, 2004.
- [14]. Dhar, s., Purohit, r., Saini, n., Sharma, a. and Kumar, G.H., 2007. Mathematical modelling of electric discharge machining of cast Al-4Cu-6Si alloy-10 wt. % sicp composites. *Journal of Materials Processing Technology*, 193(1-3), 24-29.
- [15]. Karthikeyan R, Lakshmi Narayanan, P.R. and Naagarazan, R.S., 1999. Mathematical modeling for electric discharge machining of aluminium-silicon carbide particulate composites. *Journal of Materials Processing Technology*, 87(1-3), 59-63. [3]. El-Taweel, T.A., 2009. Multi-response optimization of EDM with Al-Cu-Si-tic P/M composite electrode. *International Journal of Advanced Manufacturing Technology*, 44(1-2), 100-113.
- [16]. Mohan, B., Rajadurai, A. and Satyanarayana, K.G., 2002. Effect of sic and rotation of electrode on electric discharge machining of Al-sic composite. *Journal of Materials Processing Technology*, 124(3), 297-304.
- [17]. Lin, y.-. Cheng, C.-. Su, B.-. And Hwang, L.-. 2006. Machining characteristics and optimization of machining parameters of SKH 57 high-speed steel using electrical-discharge machining based on Taguchi method. *Materials and Manufacturing Processes*, 21(8), 922-929.
- [18]. J. Simao, H.G. Lee, D.K. Aspinwall, R.C. Dewes, and E.M. Aspinwall 2003. Workpiece surface modification using electrical discharge machining,, 43 (2003) 121– 128 .
- [19]. Yan-Cherng Lin, Yuan-fengchen, Ching-tien Lin, AND Hsinn-jyhTzeng Feasibility study of rotary electrical discharge machining with ball

- burnishing for Al₂O₃/6061Al composite 2008, vol.23: 391– 399.
- [20]. Lee, S.H. and Li, X.P., 2001. Study of the effect of machining parameters on the machining characteristics in electrical discharge machining of tungsten carbide. *Journal of Materials Processing Technology*, 115(3), 344-358.
- [21]. Hassan, El-Hoffy, *Advanced Machining Processes*, Chapter 5, pp.115- 140, by McGraw-Hill Company, 2005.
- [22]. Luis, C., J., et al, Material removal rate and electrode wear study on the EDM of silicon carbide, *Journal of Materials Processing Technology*, Vol. 164-165, pp 889-896, 2005.
- [23]. Chen, Y., and Mahdavian, S., M., Parametric study into erosion wear in a computer numerical controlled electro-discharge machining process, *Wear*, Vol. 236, pp. 350-354, 1999.
- [24]. Singh, P.N., Raghukandan, K., Rathinasabapathi, M. And Pai, B.C., 2004. Electric discharge machining of Al-10%SiCp as-cast metal matrix composites. *Journal of Materials Processing Technology*, 155-156(1-3), 1653-1657.
- [25]. Soveja, A., Cicala, E., Grevey, D. And Jouvard, J.M., 2008. Optimisation of TA6V alloy surface laser texturing using an experimental design approach. *Optics and Lasers in Engineering*, 46(9), 671-678.
- [26]. Yan, B.H., Wang, C.C., Chow, H.M. and Lin, Y.C., 2000. Feasibility study of rotary electrical discharge machining with ball burnishing for Al₂O₃/6061Al composite. *International Journal of Machine Tools and Manufacture*, 40(10), 1403-1421.
- [27]. Puertas, I. And Luis, C.J., 2004. A study of optimization of machining parameters for electrical discharge machining of boron carbide. *Materials and Manufacturing Processes*.
- [28]. Dilshad Ahmad Khan and Mohammad Hameedullah, "Effect of tool polarity on the machining characteristics in Electric Discharge Machining of silver steel and statistical Modelling of the process", *International Journal of Engineering Science and Technology (IJEST)*, Vol. 3 No. 6 June 2011, pp 5001 – 5010.

Cite this article as :

Rahul Shrinivasan, Tushar Bhakte "Review on MRR in Spark Erosion Machining (SEM) Through ANN", *International Journal of Scientific Research in Science and Technology (IJSRST)*, Online ISSN : 2395-602X, Print ISSN : 2395-6011, Volume 9 Issue 1, pp. 218-237, January-February 2022. Available at doi : <https://doi.org/10.32628/IJSRST229138> Journal URL : <https://ijsrst.com/IJSRST229138>